ARTICLE IN PRESS

Nuclear Inst. and Methods in Physics Research, A xxx (xxxx) xxxx

Contents lists available at ScienceDirect

Nuclear Inst. and Methods in Physics Research, A

journal homepage: www.elsevier.com/locate/nima

Large Area Picosecond Photodetector (LAPPD™) - Pilot production and development status

M.J. Minot [a,*], B.W. Adams [a], M. Aviles [a], J.L. Bond [a], T. Cremer [a], M.R. Foley [a], A. Lyashenko [a], M.A. Popecki [a], M.E. Stochaj [a], W.A. Worstell [a], M.J. Wetstein [b], J.W. Elam [c], A.U. Mane [c], O.H.W. Siegmund [d], C. Ertley [d], H.J. Frisch [e], A. Elagin [e], E. Angelico [e], E. Spieglan [e]

[a] *Incom, Inc, Charlton, MA, USA*
[b] *Iowa State University, United States*
[c] *Argonne National Laboratory, Lemont, IL, USA*
[d] *University of California, Berkeley, CA, USA*
[e] *University of Chicago, Chicago, IL, USA*

ARTICLE INFO

Keywords:
LAPPD
Large area photodetector
Picosecond timing
ALD MCP
Microchannel plate
Photon counting

ABSTRACT

We report performance results achieved for fully functional sealed Large Area Picosecond Photodetectors (LAPPD™) in tests performed at Incom Inc., as well as independent test results reported by our early adopters. The LAPPD is a microchannel plate (MCP) based large area picosecond photodetector, capable of imaging with single-photon sensitivity at high spatial and temporal resolutions in a hermetic package. The LAPPD has an active area of 350 square centimeters in an all-glass hermetic package with a fused silica window and bottom plate and sidewalls made of borosilicate float glass. Signals are generated by a bi-alkali Na_2KSb photocathode and amplified with a stacked chevron pair of MCPs produced by applying resistive and emissive atomic layer deposition coatings to glass capillary array (GCA) substrates. Signals are collected on RF stripline anodes applied to the bottom plates which exit the detector via pin-free hermetic seals under the side walls. LAPPD test and performance results for product produced and delivered to early adopter customers during the first half of 2018 are reviewed. These results include electron gains $\geq 7.5 \times 10^6$ @ 850/950 V (entry/exit MCP), low dark noise rates (22 Cts/s/cm^2), single photoelectron (PE) timing resolution of 64 picoseconds RMS, and single photoelectron spatial resolution along and across strips of 2.8 mm and 1.3 mm RMS respectively. Many of these devices also had very high QE photocathodes that were uniform over the full 195 mm × 195 mm window active area (LAPPD #15 QE% @ 365 nm Max/Avg/Min = 25.8/22.3 ± 3/15.7). An update is also provided of developments that enable capacitive signal coupling from the detector to application specific pads or stripline readout patterns deployed on printed circuit boards positioned beneath the tile, outside of the vacuum package. We conclude with examples of how sensors offering picosecond timing, in diverse applications can bring transformative change to detector technology and applications in future experiments.

Contents

* Corresponding author.
E-mail address: mjm@incomusa.com (M.J. Minot).

https://doi.org/10.1016/j.nima.2018.11.137
Received 27 June 2018; Received in revised form 28 November 2018; Accepted 29 November 2018
Available online xxxx
0168-9002/

1. Introduction

1.1. Relevant background

LAPPD™ R&D began in 2009 led by a collaboration of universities and national laboratories, ending in December 2012 as efforts transitioned to technology transfer for commercialization [1]. The original program was motivated by the desire to provide a technical alternative to single pixel, bulky PMTs that offered nanosecond resolution, and low magnetic field tolerance, by providing a large area, compact, flat panel, multi-pixel MCP PMT with ≤60 ps timing resolution, in a low noise, compact (length = 230 mm, width = 220 mm, thickness = 22 mm), pin free package.

In 2014 the US Department of Energy funded Incom Inc. to demonstrate a pathway for commercialization of these developments and scale-up LAPPD to industrial production.

Custom equipment and facilities were designed and implemented allowing equipment and process commissioning trials to commence in November 2015. Early commissioning trials demonstrated the ability to successfully seal LAPPD, to apply uniform high QE photocathodes over the full area of the window, to achieve high gain from the chevron pair of ALD-GCA-MCPs, and to produce saturated single PE pulse height distributions [2]. These early trials culminated in the fall of 2017 with the fabrication of fully functional LAPPDs tiles that achieved all of these goals at usable levels. While process optimization of the baseline LAPPD continues, these successes are now enabling prototype LAPPDs to be fabricated on a regular pilot production basis and to be made available to early adopter users for evaluation and test.

Advanced versions of the LAPPD are also currently under active development by Incom Inc., with our university collaborators. Most notable is a next-generation design that incorporates an anode capacitively coupled through a thin metal film deposited onto the inside bottom of the detector, to an application specific printed circuit board, positioned beneath the detector tile, outside of the vacuum package. This innovation will allow the LAPPD to be customized post-production for either stripline or pad readout, simplify connectivity, and facilitate use of LAPPD in high fluence applications.

1.2. "Next generation" MCPs

An enabling component of the LAPPD™ is a chevron pair of large area (203 mm × 203 mm) "next generation" MCPs [3,4]. Advances in material science provide an alternative to the traditional lead-glass-based MCP construction, with its problems of reduced lifetime due to ion-feedback and limitations in size and thickness due to fragility. These "next generation" large-area high performance MCPs have been enabled by the convergence of two technological breakthroughs. The first breakthrough is the ability to produce large blocks of low cost, hollow, glass capillary arrays (GCAs), with micron-sized pores, developed by Incom Inc. The proprietary Incom hollow core GCA process eliminates the need to later remove core material by chemical etching. The second breakthrough was the advent of atomic layer deposition (ALD) coating methods and materials to coat or functionalize GCAs to impart the necessary resistive and secondary emission properties, converting them into highly effective MCPs with high electronic gain and robust performance properties suitable for large area time of flight detector applications. A key advantage of the "ALD-GCA-MCP" process is the ability to independently select the optimal substrate material and to then separately apply and optimize both the resistive and emissive layers, selecting from a wide variety of material options. This is not the case for conventional "prior art" lead oxide MCPs where a single lead sub-oxide resistive and emissive layer of variable composition is developed during a hydrogen reduction forming process. Additional "ALD-GCA-MCP" processing details are available in Ref. [2].

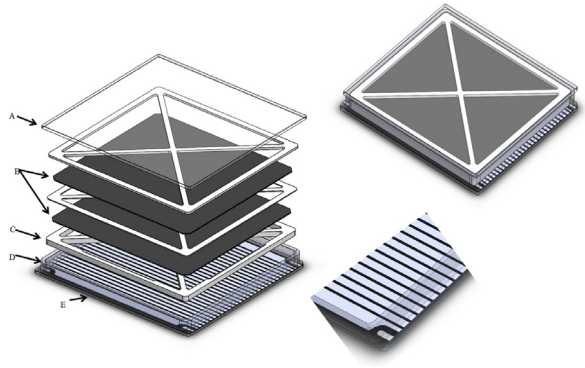

Fig. 1. Schematic design of the LAPPD.

Table 1
LAPPD #25 — General design features and parameters.

Feature	Parameter
Photodetector material	Borosilicate glass
Window material	Fused silica glass
Photocathode material	Multi-Alkali (K_2NaSb)
PC λ maximum response (nm)	380–410 nm
Active area dimensions	195 mm × 195 mm
Active fraction/area (X-spacers)	92%/34,989 mm^2
Anode data strip configuration	28 silver strips, 5.2 mm wide, 1.7 mm gap, 50 Ω impedance
Voltage distribution	5 taps — independent voltage control of PC and entry/exit MCP

1.3. LAPPD design

General design features and parameters for LAPPD #25 are shown in Table 1. A schematic, showing an exploded view of the LAPPD, with chevron pair of ALD-GCA-MCPs, X-spacer, and anode data strips is shown in Fig. 1: Left, exploded view: (A) Fused silica window with PC on inside surface, (B) Chevron pair of ALD-GCA-MCPs, (C) three spacers, (D) Anode showing 28 strip lines passing under (E) sidewalls of lower tile assembly. Top right: consolidated view, Bottom right: expanded view of strip line anodes passing under sidewalls.

2. LAPPD performance test methods

LAPPD performance tests were performed in a dark box with a UV light source and signal acquisition hardware. LAPPDs are provided with an Ultem housing that provides high voltage connections, and a backplane as shown in Fig. 2 that connects anode strips to SMA connectors with near-50 ohm impedance. Recommended high voltage connections that separate current paths of the entry and exit MCPs, allowing independent control of the photocathode and MCP voltages are shown in detail measurement & test reports available online [5]. Gain was measured as a function of MCP voltage, using a charge-sensitive amplifier and an ADC, and subsequently measured using PSI DRS4 waveform evaluation boards [6].

Photocathode QE measurements were made using a 365 nm UV LED source, illuminating a ~10 mm diameter area that was scanned in 5 mm steps across the window to create the plot shown in Fig. 3 (left).

Gain is shown as a function of MCP voltage in Fig. 4. MCP pulses for the gain measurement were produced by directing a 405 nm Edinburgh Instruments 60 pS UV pulsed laser onto to a selected point on the LAPPD window. The laser was triggered externally at 145 Hz. The trigger pulse was also used to provide a 12 μS gate window for the ADC, so the pulse height analyzer could detect charge pulses from the LAPPD response from the laser, when they occurred, with minimal inclusion of dark pulses. A neutral density filter (NE540B from Thorlabs) was used on the laser to reduce the intensity to the single photon level. Photoelectrons

Please cite this article as: M.J. Minot, B.W. Adams, M. Aviles et al., Large Area Picosecond Photodetector (LAPPD™) - Pilot production and development status, Nuclear Inst. and Methods in Physics Research, A (2018), https://doi.org/10.1016/j.nima.2018.11.137.

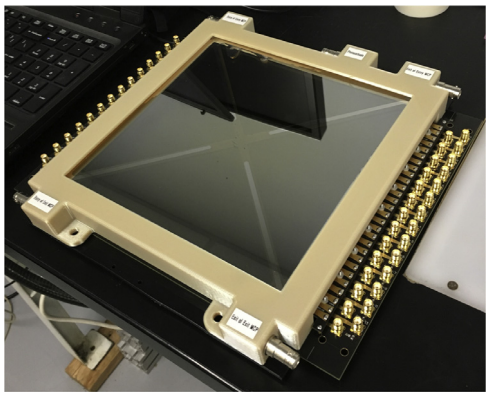

Fig. 2. LAPPD is shown enclosed in Ultem housing with high voltage connectors, mounted on a backplane for signal access.

were produced and amplified by the LAPPD for roughly 4 out of every 10 laser pulses. Gain measurements were also made using waveform sampling, where the integral sum of signal current over time for each MCP pulse is used to measure the charge in the pulse.

2.1. Charge deposition position and spatial resolution

The position of the MCP charge deposition may be measured with the LAPPD strip line anode in two ways. Along a strip, the position of the charge pulse may be determined by measuring the difference in time of arrival of pulses at each end of the strip, as the charge deposited by the MCP propagates independently to each end. Position may be measured perpendicular to the strip axes by measuring the centroid of three or more adjacent strip signals, resulting in the position to better resolution than the strip pitch.

2.2. Timing resolution

In addition to the tests completed at Incom Inc., confirming tests, and timing resolution tests were performed on LAPPD #25 at the Iowa State University, on behalf of the ANNIE collaboration [7]. ANNIE testing was done in a dark box, with motorized optics allowing for position scans, similar to Incom's. In addition however, the availability of a PiLAs laser with 30 ps RMS resolution, a 10 GHz, 20 Gs/s scope, and PSEC4 waveform digitizing electronics, enabled preliminary rise time and transit time spread testing to be performed. A single photoelectron Transit Time Variation of 64 pS was measured (Fig. 5, right).

3. Results

LAPPD #25 performance is summarized in Table 2. The average QE at 365 nm was 7.1%, with a standard deviation of 0.8%. This calculation of the mean excluded the X-spacers and the low QE region in the upper right of the map in Fig. 3, caused by shading of misplaced alkali sources during this particular PC deposition. The X-spacers are visible in the map, although not fully dark because they are 6 mm wide while the UV spot size is 10 mm in diameter. Fig. 3 right shows QE vs. wavelength, measured as a sealed tile, immediately after fabrication. Table 3 provides a summary of QE values determined for LAPPD recently fabricated at Incom Inc., and is intended to show that while the QE for Tile #25 was comparatively modest, other tiles have been fabricated with photocathodes that have met or exceeded our initial target goals of 20%.

Despite its modest photocathode QE, Tile #25 was selected for reporting here, since it provides a good balance of high performance MCPs, low noise, and is the first fully sealed LAPPD for which time resolution data was available.

Table 2
Summary of LAPPD #25 performances.

Parameter	Performance
MCP resistance, entry/exit; MΩ	14.2/10.7/MΩ at 875 V
PC QE% Max, Mean, σ	@365 nm: 10.0/7.1/0.8% @455 nm: mean = 10.2% ± 1.5
PC QE spatial variability, σ	11% of the mean
LAPPD gain	7.5×10^6 @ 850/950 V entry/exit MCP $\sigma \leq 50\%$ mean
Tile dark count rate at 875 V/MCP and 30 V on PC	22 Cts/s/cm^2
Cross-strip spatial resolution	1.3 mm RMS
Along-strip spatial resolution	2.8 mm RMS (as 37 ps)
Time resolution	64 ps resolution TTS MCP pulse rise time: 850 ps, FWHM: 1.1 ns

Table 3
QE summary for recent LAPPD.

LAPPD S/N	Maximum %	Average %	Minimum %
LAPPD #13:	23.5	18.6 ± 3.3	13.5
LAPPD #15:	25.8	22.3 ± 3.0	15.7
LAPPD #22:	14.7	10.6	
LAPPD #25:	10	7.1	
LAPPD #29:	19.6	13.0 ± 6.0	3
LAPPD #30:	22.9	17.2 ± 2.5	13
LAPPD #31:	14.0	9.8	1.1
LAPPD #36:	27.7	25.8	22.7
LAPPD #37	26.4	24.7	21.3

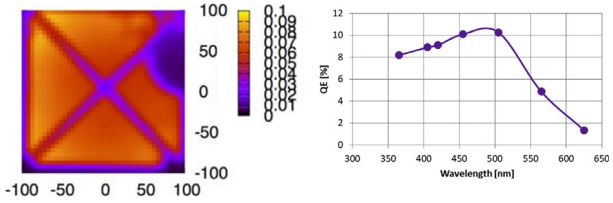

Fig. 3. Left: A PC QE map measured at 365 nm and Right: QE vs. λ.

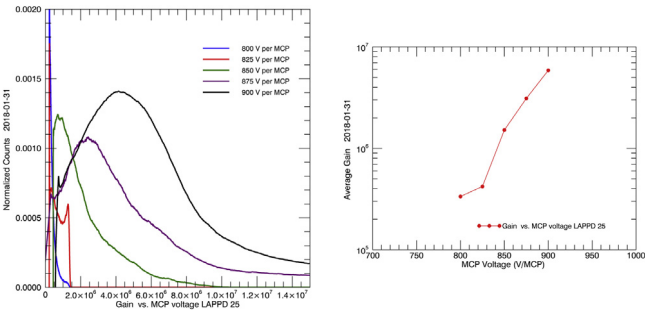

Fig. 4. Left: Pulse height distributions, Right: Average gain vs. MCP voltage as measured with a charge sensitive amplifier.

Fig. 4 (left) shows pulse height distributions vs. MCP voltage, as measured with a charge sensitive amplifier, with well peaked pulse height distributions for different voltages. Fig. 4 (right) shows average Gain vs. MCP Voltage based upon the pulse height distributions shown in the left panel. Gain was also derived from unamplified MCP pulses, using PSI DRS4 Evaluation Board devices at one MCP voltage setting. In this case, the MCPs voltages were different on the entry and exit MCPs. The gain derived with 850 V on the entry MCP and 950 V on the exit MCP and with a photoelectron extraction field of 200 V/cm was 7.9E6.

DRS4 waveform samplers were used to determine spatial resolutions for single photoelectrons scanning both along-strips as well as across-strips. The relative arrival time of pulses observed at both ends of a

Please cite this article as: M.J. Minot, B.W. Adams, M. Aviles et al., Large Area Picosecond Photodetector (LAPPD™) - Pilot production and development status, Nuclear Inst. and Methods in Physics Research, A (2018), https://doi.org/10.1016/j.nima.2018.11.137.

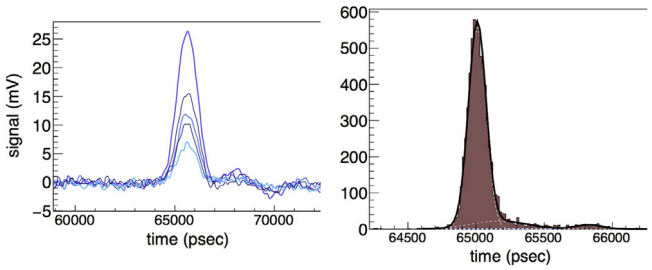

Fig. 5. Left: Typical single PE pulses are shown (FWHM: 1.1 ns, rise time: 850 ps). Single PE timing resolution of 64 ps was observed in the main peak of the transit time spread (TTS) shown on the right.

strip leads to position of charge along the strip. Timing variability at a given position provides the uncertainty of the position. For LAPPD 25, the relative arrival time sigma was 32 pS at one position. At a scale of 11.4 pS/mm this leads to a position uncertainty of 2.8 mm. Across-strip coordinates were determined from a centroid calculation that uses charge measured on three (or more) adjacent strips. The centroids were derived using the sum of the waveforms within a restricted range about the pulse peak time as a function of incident laser cross-strip position. The center of the central strip was taken as zero.

Time Resolution for LAPPD #25, measured on behalf of the ANNIE Collaboration at Iowa State University is shown in Fig. 5. Typical Single PE Pulses are shown (FWHM: 1.1 ns, rise time: 850 ps) on the left. Single PE timing resolution of 64 ps was observed in the main peak of the transit time spread (TTS).

4. Advanced development, design & optimization

Routine pilot production of the all-glass "baseline" LAPPD depicted in Figs. 1 and 2 is now underway at Incom Inc. Advanced development, testing and design optimization are also underway to address a number of performance parameters that have been identified as critical for different early adopter applications. These include (a) capacitive signal coupling from the detector to application specific pads or stripline readout patterns deployed on printed circuit boards positioned beneath the tile, outside of the vacuum package, (b) ceramic body LAPPD for applications that require a more robust tile enclosure, and (c) in-situ photocathode deposition process that promises to streamline the manufacture of LAPPD. LAPPD #36 shown in Table 3 is a fully sealed tile that incorporates the ceramic body and capacitive coupling characteristic of the GEN II LAPPD design, and a photocathode produced by the conventional transfer process.

For capacitive coupling, a thin metal DC ground plane is deposited onto the inside of the detector in place of the stripline anodes. Electrons striking the ground plane capacitively couple through the bottom plate of the detector tile to conductive pads deployed on a printed circuit board positioned outside of the tile vacuum enclosure, beneath and in-contact with the detector tile, where they are detected. Test results show that signal rise time is unaffected by capacitive coupling, and that for the geometry of the pickup board and impedance to ground used, 88% of MCP fast signal strength was capacitively coupled through the base of the tile to pads on the outside, demonstrating that sufficient signal amplitude is transferred to the pickup board for practical application [8]. Additional details of the development of ceramic sealing techniques, and in-situ photocathode deposition are given in a paper appearing in this journal [9].

5. Discussion & conclusions

The LAPPD is the newest addition to a growing family of MCP based PMTs that offer improving levels of picosecond timing now becoming available from multiple recognized photodetector vendors. In addition to large effective area, a number of features differentiate the LAPPD from currently available MCP-PMTs. LAPPD MCPs fabricated by using atomic layer deposition to apply a resistive and emissive coating to a bare glass substrate (ALD-GCA-MCP) are able to achieve much higher and more stable, low-noise gain and are expected to have much longer lifetime compared to conventional lead oxide MCPs. In the current "baseline" design configuration, strip-line anodes combined with centroiding adjacent strip signals provides a simplified approach for electronic read out while still achieving resolutions of $\lesssim$3 mm, equivalent to $\gtrsim$4900 pixels for a detector having an effective active area of 34,989 mm^2.

Multiple tiles tested at Incom Inc., as well as at Early Adopter facilities exhibit "target" performances with gain $\geq 7 \times 10^6$, PC QE $\geq$ 22%, with time and spatial resolution of $\leq$ 64 ps, and $\leq$ 3 mm respectively for single photoelectrons. The $\leq$ 64 picosecond-scale timing and mm-scale spatial resolution demonstrated for these early prototypes are for a non-optimized system and are expected to be further improved, as large area MCPs with smaller pore size ($\leq$ 10 μm) are incorporated, and adjustments to the gaps and voltages between PC/MCP1/MCP2/Anode are made. A full treatment of the variables limiting timing, and the potential that can be achieved, is available in the Refs. [10,11]. Manufacturing scale-up challenges remain to consistently achieve all of these performances in the same tile, however artifact features currently exhibited in early prototypes are expected to be resolved as production volume and experience increases. Despite these present limitations, these initial prototype tiles are providing early adopters a means to explore the full potential of pico-second-level timing.

Capacitive coupling, while still under development, will enable pixelated anodes deployed directly onto printed circuit boards outside of the tile vacuum enclosure. The ability to manufacture a universal detector tile, and to then customize the anode read-out, whether stripline, or pads, as part of a separately provided printed circuit board, is expected to significantly reduce manufacturing costs and improve performance for the customer. A number of independent firms are now developing "LAPPD read-out boards" equipped with on-board electronics. In one example under development [12] high bandwidth amplifiers are coupled to DRS4 chips to sample electrical pulses at each end of the anode strips. A Xilinx Artix-7 FPGA provides reconfigurable triggering capability and control over digitization of the DRS4 samples. The readout card can record 1024-sample full waveforms on all strip ends (28 per side, 56 total) at up to 5 GSPS. Optically isolated gigabit Ethernet readout is supported using a small form-factor pluggable (SFP) in a compact, optical module transceiver.

The availability of low cost, large area photodetectors that offer picosecond-scale timing is expected to have a transformative effect on the way future experiments will be conducted. In March 2018, a "Fermilab-University of Chicago" Picosecond Timing Meeting was held to explore new opportunities that could be enabled by PSEC timing. Multiple applications were identified for particle detection in accelerator physics, collider physics, neutrinoless double beta decay and nuclear physics [13–16]. In one application [17], mirrors and picosecond timing were used to effectively double the photo-detection efficiency while providing a time-resolved image of the Cherenkov light on the opposing wall. It is expected that as end users become more familiar with the benefits of picosecond-level timing, these applications will grow.

Acknowledgments

This work supported by U.S. Department of Energy, USA, Office of Science, USA, Office of Basic Energy Sciences, USA, Offices of High Energy Physics, USA and Nuclear Physics, USA under DOE contracts: DE-SC0009717; DE-SC0011262, and DE-SC0015267.

Please cite this article as: M.J. Minot, B.W. Adams, M. Aviles et al., Large Area Picosecond Photodetector (LAPPD™) - Pilot production and development status, Nuclear Inst. and Methods in Physics Research, A (2018), https://doi.org/10.1016/j.nima.2018.11.137.

References

[1] H.J. Frisch, et al., A Brief Technical History of the Large-Area Picosecond Photodetector (LAPPD) Collaboration, https://arXiv:1603.01843.
[2] M.J. Minot, et al., Pilot production & commercialization of LAPPD™, Nucl. Instrum. Methods A 787 (2015) 78–84.
[3] J.W. Elam, A.U. Mane, J.A. Libera, J.N. Hryn, O.H.W. Siegmund, Jason McPhate, M.J. Wetstein, A. Elagin, M.J. Minot, A. O'Mahony, R.G. Wagner, W.M. Tong, A.D. Brodie, M.A. McCord, C.F. Bevis, Synthesis, characterization, and application of tunable resistance coatings prepared by atomic layer deposition, ECS Trans. 58 (10) (2013) 249–261.
[4] US Patent: Tunable Resistance Coatings; US Patent Number 8, 921, 799 B2, Issued December 30, 2014; US Patent Number 9, 105, 379 B2, issued August 11, 2015 Inventors: Jeffrey W. Elam, Anil U. Mane.
[5] http://www.incomusa.com/mcp-and-lappd-documents/.
[6] https://www.psi.ch/drs/evaluation-board.
[7] http://annie.fnal.gov/.
[8] E. Angelico, T. Seiss, et al., Capacitively coupled pickup in MCP-based photodetectors using a conductive metallic anode, Nucl. Instrum. Methods Phys. Res. A846 (2017) 75.
[9] E. Angelico, A. Elagin, H.J. Frisch, E. Spieglan, The 'Gen-II' LAPPD™ : Large-Area Ceramic-Body Planar MCP-based Photo-Detectors, appearing in this journal.
[10] B.W. Adams, et al., Timing characteristics of LAPPD NIM, Phys. Res. A 795 (2015) 1–11.
[11] http://psec.uchicago.edu/workshops/fast_timing_conf_2011/system/docs/18/original/ritt_analog_bw.ppt.
[12] http://www.ultralytics.com.
[13] A.R. Back, et al., Accelerator Neutrino Neutron Interaction Experiment (ANNIE): Preliminary Results and Physics Phase Proposal, arXiv:1707.08222.
[14] A. Elagin, et al., Separating double-beta decay events from solar neutrino interactions in a kiloton-scale liquid scintillator detector by fast timing, Nucl. Instrum. Methods Phys. Res. A849 (2017) 102.
[15] C. Aberle, A. Elagin, H.J. Frisch, M.J. Wetstein, L. Winslow, Measuring directionality in double-beta decay and neutrino interactions with kiloton-scale scintillation detectors, JINST 9 (2014) P06012.
[16] J. Caravaca, et al., Probing cherenkov and scintillation light separation for next-generation neutrino detectors, J. Phys. Conf. Ser. 888 (1) (2017) 012056.
[17] E. Oberla, H.J. Frisch, The design and performance of a prototype water Cherenkov optical time-projection chamber, NIM 814 (2016) https://arxiv.org/abs/1510.00947.

Please cite this article as: M.J. Minot, B.W. Adams, M. Aviles et al., Large Area Picosecond Photodetector (LAPPD™) - Pilot production and development status, Nuclear Inst. and Methods in Physics Research, A (2018), https://doi.org/10.1016/j.nima.2018.11.137.